# Modeling osteosarcoma progression by measuring the connectivity dynamics using an inference of multiple differential modules algorithm

BIN LIU[1*], ZHI ZHANG[2*], E-NUO DAI[2], JIA-XIN TIAN[2], JIANG-ZE XIN[3] and LIANG XU[2]

Departments of [1]Traditional Chinese Medical Orthopedics, [2]Orthopedics and [3]Medical Oncology,
Affiliated Hospital of Shandong Academy of Medical Sciences, Jinan, Shandong 250031, P.R. China

**Abstract.** Understanding the dynamic changes in connectivity of molecular pathways is important for determining disease prognosis. Thus, the current study used an inference of multiple differential modules (iMDM) algorithm to identify the connectivity changes of sub-network to predict the progression of osteosarcoma (OS) based on the microarray data of OS at four Huvos grades. Initially, multiple differential co-expression networks (M-DCNs) were constructed, and weight values were assigned for each edge, followed by detection of seed genes in M-DCNs according to the topological properties. Using these seed gene as a start, an iMDM algorithm was utilized to identify the multiple candidate modules. The statistical significance was determined to select multiple differential modules (M-DMs) based on the null score distribution of candidate modules generated using randomized networks. Additionally, the significance of Module Connectivity Dynamic Score (MCDS) to quantify the dynamic change of M-DMs connectivity. Further, DAVID was employed for KEGG pathway enrichment analysis of genes in dynamic modules. In addition to the basal condition, four conditions, OS grade 1-4, were also included (M=4). In total, 4 DCNs were constructed, and each of them included 2,138 edges and 272 nodes. A total of 13 genes were identified and termed 'seed genes' based on the z-score distribution of 272 nodes in DCNs. Following the module search, module refinement and statistical significance analysis, a total of four 4-DMs (modules 1, 2, 3 and 4) were identified. Only one significant 4-DM (module 3 in the DCNs of grade 1, 2, 3 and 4 OS) with dynamic changes was detected

when the MCDS of real 4-DMs were compared to a null distribution of MCDS of random 4-DMs. Notably, the genes of the dynamic module (module 3) were enriched in two significant pathway terms, ubiquitin-mediated proteolysis and ribosome. The seed genes with the highest degrees included protein phosphatase 1 regulatory subunit 12A (PPP1R12A), UTP3, small subunit processome component homolog (UTP3), prostaglandin E synthase 3 (PTGES3). Thus, pathway functions (ubiquitin-mediated proteolysis and ribosome) and several seed genes (PPP1R12A, UTP3, and PTGES3) in the dynamic module 3 may be associated with the progression of OS and may serve as potential therapeutic targets in OS.

## Introduction

Osteosarcoma (OS), as an aggressive malignant cancer, is the most frequent human primary bone neoplasm in children and in adolescents (1). Notably, OS has a high metastatic potential (2). Based on the available literature, ~45% patients with OS progressed to lung metastasis, which is the major cause of death in patients with OS (3). Currently, the standard therapy is radical surgery combined with chemotherapy (4). However, there is strong controversy over the role of chemotherapy in treating cancer. Further progress is required in the treatment of OS (5). Therefore, it is urgent to investigate the detailed molecular mechanisms underlying OS progression, which will facilitate the development of effective therapeutic strategies.

Many complex diseases, for example, cancer, involve a continuum of molecular events, which begin with early initiation events and progress to disastrous end-stage events. Understanding the disease-stage-specific molecular events is vital for understanding disease pathology and developing efficient therapeutic strategies. Identification of disease-associated signatures can contribute to investigations into the process of tumorigenesis. However, it is difficult to identify novel biomarkers associated with OS, due to high costs and time-consuming experiments (6). Computational methodologies counteract this. However, the majority of computational methods focus on the differential expression of genes and static regulation between genes (7,8), ignoring the network rewiring or dynamic regulation between molecules during different disease stages. Furthermore, it is well established that many

diseases are induced by perturbations of complex molecular networks, rather than the individual genes. Differential network analysis has been applied to protein-protein interaction networks (9), protein-gene interaction networks (10), and functional gene interaction networks (11). However, only two conditions were considered (i.e., only one resulting differential network) in the former studies using computational methods. Generally, the interactions vary at different disease stages, and the changes in interactions are causally associated with disease progression. Thus, simultaneously analyzing network dynamics in the period of disease progression is of great importance for understanding disease mechanisms.

The current study attempted to detect dynamically controlled genes and modules associated with OS using a novel computational method. Inference of multiple differential modules (*i*MDM) (12) was presented to measure OS microarray data at four Huvos grades (13) to capture the connectivity changes of sub-networks during the process of OS development. Using *i*MDM, multiple sub-networks were constructed from time-course transcription data, and candidate genes that may underlie the OS were identified. Gene expression profile data of OS from the European Molecular Biology Laboratory-European Bioinformatics Institute (EMBL-EBI) database. The construction of multiple differential co-expression networks (M-DCNs) was performed using gene expression profiles across different OS conditions (grade 1, 2, 3 and 4 OS). Subsequently, *i*MDM was used to analyze the DCNs to identify shared candidate modules across different disease stages. Then, statistical analysis was performed to select multiple differential modules (M-DMs) based on the null score distribution of candidate modules generated using randomized networks. Finally, Module Connectivity Dynamic Score (MCDS) was employed to quantify the change in the connectivity of shared gene modules among different conditions. It is believed that the findings of the current study may provide guidelines for experimental validation in the future, and shed light on the pathogenesis of OS.

**Materials and methods**

*Analysis of microarray data*. The gene expression profile of E-GEOD-33382 (13) was downloaded from the EMBL-EBI database, which was based on the A-GEOD-10295 Illumina human-6 v2.0 expression beadchip platform (using nuIDs as identifier). Gene microarray data of 45 OS samples (10 OS with grade 1, 13 with grade 2, 15 with grade 3, and 7 with grade 4) with 2 replicates, and osteoblast cell samples derived from mesenchymal stem cells (n=3) in duplicate as controls were obtained. Probe annotation files were downloaded. The probes were aligned to the gene symbols, and 13,326 genes were ultimately obtained.

*STRING protein-protein interactions*. The original human protein-protein interaction network (PPIN) involving 787,896 interactions (16,730 genes) was downloaded from the STRING database (http://string-db.org/), and only the proteins that were common with the microarray data were used to construct the background PPIN.

*i*MDM approach*. A flowchart of the *i*MDM algorithm is presented in Fig. 1. This method used the input transcriptome

data gathered in control and disease conditions. The following three steps were performed: Construction of the M-DCNs, one for each condition; using the M-module algorithm (14) to extract statistically significant M-DMs in M-DCNs; quantification of the change in the connectivity of shared M-DMs.

*Construction of DCNs*. For each disease grade, the DCN was constructed on the basis of differential expression in the OS and control conditions via two steps.

In step 1, a binary co-expression network construction was implemented after edges were selected according to the absolute value of the Pearson correlation coefficient (PCC) of the microarray profiles of two genes. The 1st order partial PCC was utilized to remove indirect correlation induced by a third gene (15). In the current study, only edges with correlations greater than the predefined value $\delta(\delta=0.9)$ were reserved to construct the co-expression network.

In the second step, weight was assigned to the edge of the binary co-expression network according to the P-values of differential gene expression in the OS and control conditions. A one-side t-test was used to seek differential gene expression for microarray data. The weight $w_{x,y}$ on edge (x,y) in the DCN was defined:

$$w_{x,y} = \begin{cases} \dfrac{(\log P_x + \log P_y)^{1/2}}{(2*\max_{l\in V}|\log P_l|)^{1/2}}, & \text{if } \mathrm{cor}(x,y) \geq \delta, \\ 0, & \text{if } \mathrm{cor}(x,y) < \delta, \end{cases}$$

In this formula, $P_x$ and $P_y$ were the P-values for gene x and gene y, respectively. V was the nodes of the co-expression network, and cor(x,y) was the absolute value of PCC between gene x and gene y on the basis of their expression profiles. Under the weighting, genes that were co-expressed and markedly differentially expressed were assigned higher weight values.

Considering M-DCNs, there were the same nodes, yet edges were different and defined as $H_k=(V,E_k)$ $(1\leq k\leq M)$. A multiple candidate module, C, was determined as a set of nodes whose connectivity among them was higher than random expectation across all M-DCNs under consideration.

*Identification of multiple candidate modules in M-DCNs*. Unique and shared modules were identified across the M-DCNs, termed multiple candidate modules. The M-module algorithm described by Ma *et al* (14) is designed to extract gene modules that have common members, yet different connectivity across multiple interaction networks. Based on this, this M-module algorithm was adapted to detect the candidate modules. The identification of candidate modules consisted of three steps: i) Seed prioritization; ii) module search through seed expansion; and iii) refinement of candidate modules.

*Seed prioritization*. With the aim of identifying seed genes, genes were sorted in the M-DCNs based on the topological measurement (degree) feature. For each network $H_k=(V,E_k)$ $(1\leq k\leq M)$ with an adjacency matrix $A_k=(a_{xyk})_{n*n}$, a function was constructed to compute the importance of vertex x in the corresponding DCN, and this function was defined as:

$$g(x) = \sum_{y\in N_k(x)} A'_{xyk} g(y)$$

Where g(x) denoted the importance of vertex x in the DCN, $N_k(x)$ denotes the set of neighbors of gene x in $H_k$; $A'_k$ was the degree normalized weighted adjacency matrix which was counted as $A'_k=D^{-1/2}A_kD^{1/2}$ where D was diagonal matrix with element $D_{xy}=\sum_y A_{xyk}$. $A \cdot g$ was on behalf of the information propagation on network through the edges of networks, which meant the importance of a node depending on the number of the adjacent nodes, strength of connection and importance of its adjacent nodes.

For each gene, after acquiring its ranks in all individual DCNs, determined as $g=[g^{(1)},...,g^{(M)}]$, a z-score was calculated for each rank $g^{(1)}$. Subsequently, the sort order was obtained for that gene across all DCNs by means of averaging the z-scores among all DCNs. The top 5% genes were identified, and named as seed genes.

*Module search.* Beginning with each seed gene, the stage of module search iteratively contained genes whose addition resulted in the maximum decrease in the graph entropy-based function till no decrease was observed in the objective function. For a given vertex $x \in C$, $L_k(x)$ was denoted as the total weight between vertex x as well as other vertices of the candidate module C in the network $H_k$. Similarly, $\bar{L}_k(i)$ represented the weight value between vertex x as well as vertices outside of module C. Then, the entropy for connectivity of vertex x to module C was:

$$G_k(C_x) = -p_x^{[k]}\log p_x^{[k]} - (1-p_x^{[k]})\log(1-p_x^{[k]})$$

$$p_x^{[k]} = \frac{L_k(x)}{\bar{L}_k(i) + L_k(x)}$$

The objective for using graph entropy was to quantify the skewness of in-module connectivity vs. out-module connectivity. Adding over all vertices in C and DCN k, the entropy for C across all DCNs and normalized for the size of C was shown as follows:

$$G(C) = \frac{(\sum_{k-1}^M G_k(C))}{|C|}$$

Where $Gk(C) = \sum_{x \in C} H(C_y)$.

The objective function was defined as:

$$\sum_{x=1}^\tau \min H(C_x)$$

$$s.t. \{i_{xy} \in \{0,1\}; \sum_{y=1}^\tau i_{xy} \geq 1; \sum_{x=1}^n i_{xy} > 0$$

Where $C_x$ $(1<x<\tau)$ is a candidate module. $i=[i_1,...,i_\tau]$ was an index matrix where each column was a module and each row equaled to a gene. The constraint was that each gene belonged to one or more modules, and each module has to include at least one gene.

*Refinement of candidate modules.* During the refinement step, the multiple candidate modules with sizes <5 were eliminated. Furthermore, the Jaccard index (16), which is the ratio of intersection over union for two sets, was employed to merge the overlapping multiple candidate modules. In the current study, a Jaccard index ≥0.5 was set as the threshold.

*Statistical significance of candidate modules.* In this study, the statistical significance of multiple candidate modules was performed based on the null score distribution of candidate modules generated using randomized networks. Briefly, each network was randomized 100 times by degree-preserved edge shuffling. In order to require the module scores for the null distribution, module search was implemented on the randomized networks. Significantly, the empirical P-value of a candidate module was counted as the probability of the module having the observed score or smaller by chance using the formula below:

$$P\ value = \frac{sum\ (count\ (H_R) > count\ (H_{DCN}))}{count\ (H_R)}$$

In which count $(H_R)$ stood for the number of modules produced by randomized networks, count $(H_{DCN})$ represented the number of modules generated by DCN.

Then, P-values were adjusted for multiple testing using false discovery rate (FDR) based on the method of Benjamini-Hochberg (17). FDR≤0.05 was set as the significance threshold.

*Quantification of connectivity dynamics of shared M-DMs.* By definition, each M-DM with M≥2 has multiple component modules from different DCNs. In an attempt to quantify the connectivity change of component modules, the MCDS as a graph-theoretical measure was used. In detail, given an M-DMC whose weighted adjacent matrices of the corresponding induced subgraphs were denoted by $A_X^C(1\leq x\leq M)$, the MCDS between two adjacent component modules was determined as the $L_2$ norm of the matrix subtraction normalized by the number of genes in the M-DM. The overall MCDS of an M-DM is defined as the mean MCDS of all pairwise comparisons, and computed based on the equation:

$$\tau(A^C) = \sum_{x=1}^{M-1} \Delta A_{x,x+1}^C/(M-1)$$

Similarly, the statistical significance of MCDS for an M-DM was calculated as that for M-DMs. Specifically, the null distribution for MCDS scores was firstly counted on the basis of the random M-DMs. Then, the P-value of an MCDS was calculated based on the null distribution. Finally, the Benjamini-Hochberg was applied for correction. A FDR of 0.05 was considered as the significance threshold.

In order to identify dynamically controlled genes in OS, topological parameters were utilized to deeply investigate biological significance of genes in dynamic module.

*Pathway enrichment analysis for the genes in dynamic modules identified.* Previously, several studies have demonstrated that certain pathways are more dynamic than others in the progression of disease (18,19). To reveal this, in the present study, Database for Annotation, Visualization and Integrated Discovery (DAVID; version 6.8; https://david.ncifcrf.gov) (20,21) was employed for Kyoto Encyclopedia of Genes and Genomes (KEGG; http://www.genome.jp/kegg) pathway enrichment analysis of genes in dynamic modules obtained above, which provides analytic tools for extracting
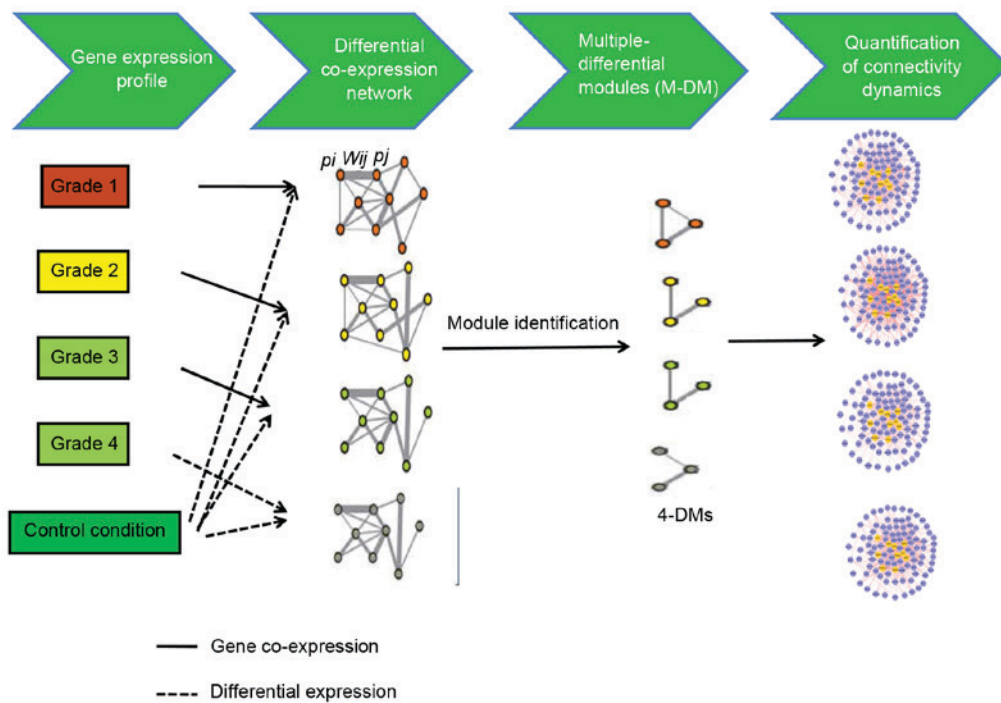
Figure 1. Summary of the inference of multiple differential modules approach. This approach includes two main steps. In the first step, differential gene co-expression networks are constructed using microarray data across multiple conditions. To construct differential gene co-expression networks, a binary co-expression network is built where edges are selected according to the absolute value of Pearson correlation coefficient of the expression profiles of two genes. Only edges with correlation higher than the pre-defined threshold δ are chosen in the co-expression network. Then, edges in the binary co-expression network are weighted ($W_{x,y}$) on the basis of the P-values ($P_x$ and $P_y$) of differential gene expression between control and disease conditions. During the second step, multiple differential gene co-expression networks are analyzed to extract shared multiple differential modules across different conditions. multiple differential modules with M=4 are the modules that are screened out under 4 conditions (grade 1, 2, 3, and 4 osteosarcoma).

biological meaning from large list of genes (20). Expression Analysis Systematic Explorer (EASE) was utilized to evaluate the significant pathways. Significant terms were determined according to the presence of at least two genes and P<0.05 in the pathways.

## Results

*M-DCNs construction*. In our study, in addition to basal conditions, four conditions, OS grades 1-4, were also included (M=4). Thus, 4 DCNs would be acquired, and identify 4-DMs. Subsequently, the significance of DMs and MCDS was used to further extract significant genes. These significant genes across four conditions may shed light on the molecular mechanism underlying OS progression in different grades.

The microarray data were aligned to the original PPIN, then the background PPIN was identified, which contained 400,797 interactions and 11,863 genes. In order to eliminate indirect correlations and to make this network more confident, only interactions with δ≥0.9 in the background PPIN were selected to construct DCNs, Thus, 4 DCNs were constructed, and each of them included 2,138 edges and 272 nodes.

*Identification of multiple candidate modules in-M DCNs and statistical significance of candidate modules*. Based on the z-score distribution of 272 nodes in DCNs, 13 genes had top 5% z-score value, which were termed as seed genes (Table I). The z-scores of all seed genes were >200. Subsequently, the

steps of module search and module refinement were implemented. Subsequently, 4 candidate modules in the DCNs of all grade 1, 2, 3, and 4 OS conditions were screened out.

Next, empirical P-values of these 4 candidate modules were calculated using randomized networks. At a FDR criterion of 0.05, these 4 candidate modules including module 1, 2, 3 and 4 were significant, as presented in Table II.

*Shared 4-DMs can be utilized to uncover dynamics in the process of OS progression*. Since component modules of a 4-DM had the same gene set in M-DCNs, yet were different in the connectivity, 4-DM offers a natural way to obtain the changes in dynamic connectivity. Thus, to this end, MCDS were used to quantify the dynamics of 4-DMs in the current study. Because the DCNs were weighted on the basis of the degree of gene expression correlation, MCDS quantified not only the presence and absence of edges, but also the changes in edge weights, which can be regarded as the interaction strength among genes.

In order to extract M-DMs that exhibit significantly different dynamics than would be expected by chance, the MCDS of real 4-DMs were compared to a null distribution of MCDS of random 4-DMs. At an FDR-value threshold of 0.05, only module 3 observed in the DCNs of grade 1, 2, 3 and 4 OS was dynamic. This dynamic DM involved 103 nodes and 870 edges, as presented in Fig. 2. As OS progression increased, the connectivity of multiple interactions in this module was markedly changed, which indicated that network rewiring has important roles during OS progression.

Table I. Seed genes and the distribution of their average z-scores.

| Gene name (gene symbol) | Average z-score |
| --- | --- |
| Karyopherin subunit α 3 (KPNA3) | 354.1070 |
| UTP3, small subunit processome component homolog (UTP3) | 304.5631 |
| Asparaginyl-tRNA synthetase (NARS) | 273.5091 |
| Prostaglandin E synthase 3 (PTGES3) | 268.3388 |
| ARP6 actin-related protein 6 homolog (ACTR6) | 256.8489 |
| ALG5, dolichyl-phosphate β-glucosyltransferase (ALG5) | 233.6674 |
| Protein phosphatase 1 regulatory subunit 12A (PPP1R12A) | 229.4946 |
| Ubiquitination factor E4A (UBE4A) | 227.2643 |
| Immediate early response 3 interacting protein 1 (IER3IP1) | 219.0473 |
| YEATS domain containing 4 (YEATS4) | 209.6316 |
| Chromosome 14 open reading frame 166 (C14orf166) | 207.9445 |
| Activating transcription factor 1 (ATF1) | 207.7166 |
| RAP1B, member of RAS oncogene family (RAP1B) | 205.7397 |

Table II. The significant modules based on FDR.

| Modules | FDR values | Nodes | Edges | Initial seed gene |
| --- | --- | --- | --- | --- |
| Module 1 | 0 | 166 | 1731 | KPNA3 |
| Module 2 | 9.78E-03 | 140 | 1539 | UTP3 |
| Module 3 | 0 | 103 | 870 | PPP1R12A |
| Module 4 | 0 | 71 | 578 | YEATS4 |

FDR, false discovery rate; KPNA, karyopherin subunit α 3; UTP3, UTP3 small subunit processome component homolog; PPP1R12A, protein phosphatase 1 regulatory subunit 12A; YEATS4, YEATS domain containing 4.

Since the edge weight in DCNs is a degree of differential expression between disease and control conditions, the mean edge weight serves as a measure of differential activity of the module. Fig. 3 presents the distribution of edge weight in the dynamic 4-DMs for grade 1, 2, 3 and 4 OS. For the sake of clarity, only edges that had significant weight changes ($P<0.05$) were exhibited. As presented in Fig. 3A, the number of interactions in the grade 4 OS network was greater than that in the other networks in the weight distribution of 0.1-0.2; particularly higher compared with grade 1 and 2 OS networks. Furthermore, the count of interactions in grade 2 OS network was greater than that in other networks in the weight distribution of 0.3-0.5. Similarly, the number of interactions in grade 3 OS network was higher in the distribution of 0.2-0.3, relative to the other conditions.

For this dynamic module, the majority of the changed edges with increased weight were detected in the grade 2 OS, relative to the other three OS conditions (Fig. 3B). Accordingly, these connectivity changes demonstrated that the pathway was rewired between different OS grades.

By analyzing the topological centrality (degree) for genes, if was determined that seed genes, including protein phosphatase 1 regulatory subunit 12A (PPP1R12A), UTP3, small subunit processome component homolog (UTP3), prostaglandin E synthase 3 (PTGES3) and ubiquitination factor E4A had the highest degrees among the genes.

*Pathway enrichment analysis.* Previously, several studies have demonstrated that certain pathways are more dynamic than others during the progression of disease (18,19). To investigate this in OS, pathway enrichment analysis was performed for dynamic module 3. Based on the presence of at least two genes and a $P<0.05$ in the pathways, a total of two significant pathway terms (ubiquitin-mediated proteolysis and ribosome) were identified to be enriched in this module.

**Discussion**

From a biological perspective, numerous diseases are induced by perturbations to the gene network. Such perturbations change dynamically as the disease develops. However, the knowledge about the dynamics of gene networks in the process of disease progression is rather limited. Thus, in the current study, an *i*MDM algorithm was created to analyze the microarray data from OS at four clinical stages to capture the connectivity changes of sub-networks in the process of OS development, and to identify candidate genes that may be useful for OS treatment. Based on the z-score distribution of 272 nodes in DCNs, 13 seed genes were identified. Following the determination of statistical significance of multiple candidate modules, a total of four candidate modules, modules 1, 2, 3 and 4, were significant. Furthermore, module 3 observed in the DCNs of grade 1, 2, 3 and 4 OS were dynamic when the MCDS of real 4-DMs were compared with a null distribution of MCDS of random 4-DMs. The initial seed gene of this module was PPP1R12A. Notably, the functions of the dynamic module 3 included ubiquitin-mediated proteolysis and ribosome. Seed genes with the highest degrees included PPP1R12A, UTP3 and PTGES3. The results demonstrated that pathway functions (ubiquitin-mediated proteolysis and ribosome) and several seed genes (PPP1R12A, UTP3 and PTGES3) may have important roles in the progression of OS.

The ubiquitin-mediated proteolysis system has important functions in various basic cellular processes, for instance regulation of cell cycle, immune and inflammatory responses, modulation of development and differentiation (22). Considering its role in numerous processes, it is unsurprising that ubiquitin-mediated proteolysis has been implicated in the progression of various diseases. Alterations in ubiquitin-mediated proteolysis has been suggested to be significantly associated with overexpression of hypoxia inducible factor (HIF)-1α and HIF-2α (23). Notably, HIF-1α has been demonstrated to induce a hypoxic microenvironment
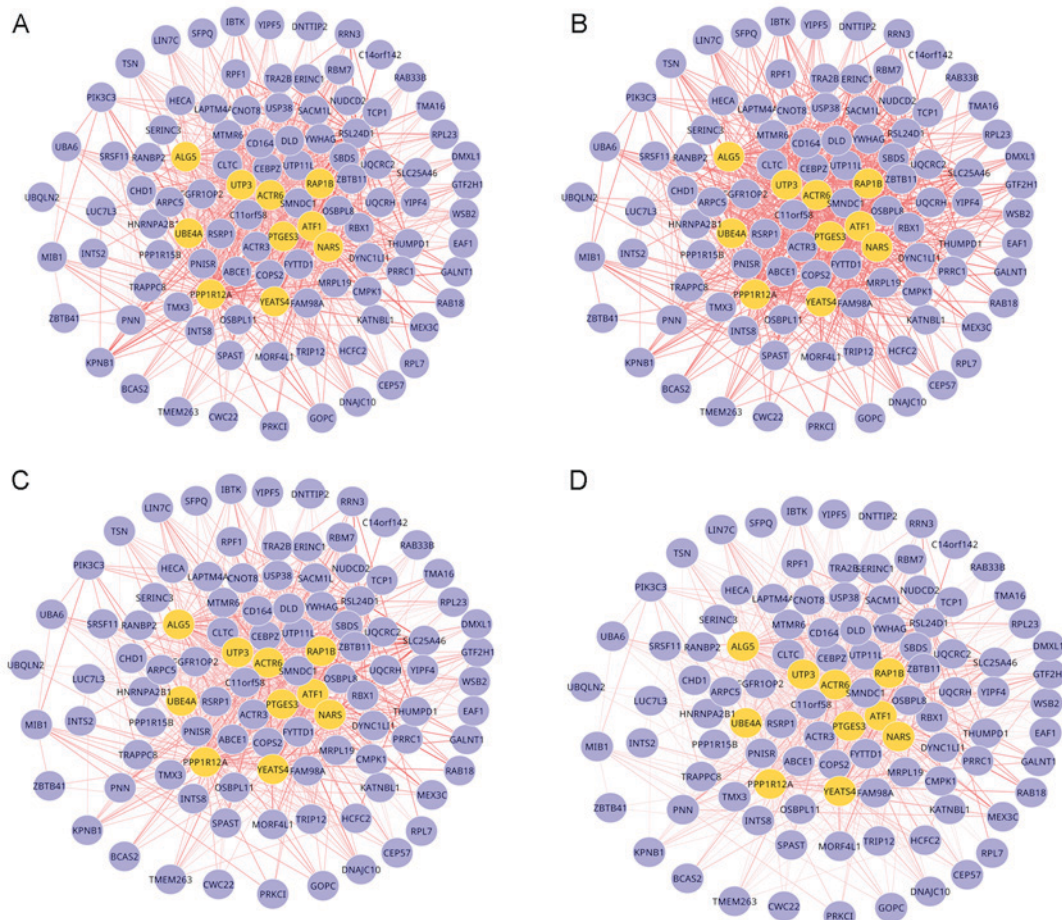
Figure 2. One dynamics 4-DMs extracted from DCNs, each of which contained 103 nodes and 870 edges. (A) A 4-DM identified in grade 1 OS and control DCNs. (B) A 4-DM identified in grade 2 OS and control DCNs. (C) A 4-DM identified in grade 3 OS and control DCNs. (D) A 4-DM identified in grade 4 OS and control DCNs. Only edges showing significant changes in edge weights between the four DCNs were exhibited. Edge thickness is proportional to the absolute value of difference of Pearson correlation coefficient of two genes. Difference was counted as 'OS-control'. Unconnected nodes demonstrated that there was no edge connected to the nodes that displayed significance change in weight value between the two conditions. Yellow nodes are the seed genes. DM, differential module; DCN, differential co-expression network; OS, osteosarcoma.
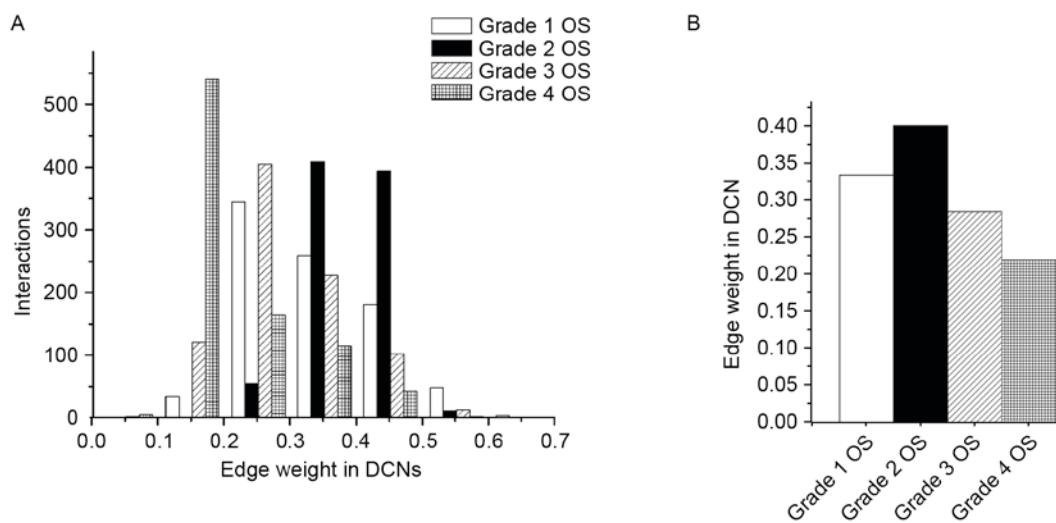


Figure 3. (A) Distribution for edge weight of identified dynamic modules. (B) Histograms of the edge weight for dynamic 4-differential modules in the respective networks. DCN, differential co-expression network; OS, osteosarcoma.

via coordinated regulation of hypoxia-responsive genes, and adaptation to a hypoxic microenvironment is crucial for the tumor progression (24). Additionally, Guo *et al* (25) have indicated that HIF-1α is activated in human OS. Thus, it is inferred

that the ubiquitin-mediated proteolysis pathway may have an important role in OS progression.

PPP1R12A, a member of myosin phosphatase target (MYPT) family, is also termed MYPT1. PPP1R12A is part of a Rho kinase pathway (26). As previously reported, PPP1R12A participates in diverse cellular functions, including cell cycle regulation (27,28), and cell migration and adhesion (29). In cancer cells, abnormal regulation of cell division contributes to metastatic potential (30). It is demonstrated that the cell cycle regulatory pathway is often somatically inactivated in OS (31). Furthermore, suppression of Notch signaling inhibits OS growth by changing the expression of cell cycle regulators (32). Cell migration is a multistep process that requires alterations of cell-substrate adhesions, cytoskeleton and extracellular matrix. Aberrant migration is associated with inflammatory disorders and cancer (33-35). Specifically, 82% pancreatic cancers have enhanced expression of PPP1R12A (36). Currently, knowledge of the involvement of PPP1R12A in OS progression is limited. In light of these results, we hypothesize that PPP1R12A may be a potential gene involved OS progression, partially via altered regulation of the cell cycle and cell migration.

UTP3 is a component of the small subunit (SSU) processome. The SSU processome, consisting of 40 proteins and the U3 small nucleolar RNA, is required for ribosome biosynthesis (37). Ribosomes are vital for the translation of mRNA into protein and are essential for cell growth. Dysregulation of ribosome biosynthesis has been indicated to be connected with alterations in cell proliferation, cell cycle and cell growth (38,39). Changing the dynamics of ribosome production can frequently accelerate cell transformation and contribute to increased susceptibility to cancer (40). Furthermore, Jorgensen et al (41) used microarray data to demonstrated that deletion of UTP4, UTP6, and UTP10, which are all involved in ribosome biogenesis, suppresses cancer cell proliferation. Bernstein and Baserga (42) indicated that when SSU processome proteins are detected, ribosomes are no longer generated and cells stall in G1. In the current study, dynamic module 3, which was observed in all grade 1, 2, 3, and 4 OS DCNs, was enriched for genes involved in the ribosome pathway. Accordingly, it is inferred that UTP3 may have important roles in OS development via regulating ribosome biogenesis, which further mediates cell cycle progression.

PTGES3 is a prostaglandin E synthase enzyme. Dysregulation of the prostaglandin-endoperoxide synthase pathway may cause the accumulation of pro-inflammatory signals, which is characteristic of cancer (43,44). Recently, PTGES3 has been suggested to be overexpressed in multiple cancers, including colorectal (45) and non-small cell lung cancer (46). Notably, a previous study demonstrated that the high expression of PTGES3 is associated with the stage of endometrioid endometrial cancer (47). Taken together, the findings of the current study indicate that PTGES3 may affect the progression of OS by regulating inflammatory responses.

In conclusion, the data of the present study offers a comprehensive bioinformatics analysis of OS, which may provide new insights into the understanding of the mechanism underlying OS progression. There are multiple directions whereby the *i*MDM concept can be extended in future work. For instance, genetic mutation data from exomes can be applied as prior information to guide module searching, under the hypothesis that mutated sequences are potentially involved in the diseases being investigated. In addition, transcriptome information can be integrated with epigenomic data to understand how environmental factors disrupt gene networks. Furthermore, comparing dynamic events referring to different molecular types may provide new mechanistic insights into the interactions in the progression of disease. Finally, the *i*MDM framework is widely applicable to other tumor samples for which disease stage-specific transcriptome data are available. The genes and pathways identified using *i*MDM may be used as potential biomarkers in clinics. Thus, in the current study, pathway functions (ubiquitin-mediated proteolysis and ribosome) and several seed genes (PPP1R12A, UTP3, and PTGES3) in the dynamic module (module 3) are associated with the progression of OS and may serve as potential therapeutic targets in this disease. Nevertheless, further experimental studies are still required to verify these findings.

## References

1. Ottaviani G and Jaffe N: The epidemiology of osteosarcoma. In: Pediatric and adolescent osteosarcoma. Springer, pp3-13, 2010.
2. Walkley CR, Qudsi R, Sankaran VG, Perry JA, Gostissa M, Roth SI, Rodda SJ, Snay E, Dunning P, Fahey FH, *et al*: Conditional mouse osteosarcoma, dependent on p53 loss and potentiated by loss of Rb, mimics the human disease. Genes Dev 22: 1662-1676, 2008.
3. Buddingh EP, Anninga JK, Versteegh MI, Taminiau AH, Egeler RM, van Rijswijk CS, Hogendoorn PC, Lankester AC and Gelderblom H: Prognostic factors in pulmonary metastasized high-grade osteosarcoma. Pediatr Blood Cancer 54: 216-221, 2010.
4. Rettew AN, Getty PJ and Greenfield EM: Receptor tyrosine kinases in osteosarcoma: Not just the usual suspects. In: Current Advances in Osteosarcoma Springer, pp47-66, 2014.
5. Hameed M and Dorfman H: Primary malignant bone tumors-recent developments. In: Seminars in diagnostic pathology. Elsevier, pp86-101, 2011.
6. Polager S and Ginsberg D: p53 and E2f: Partners in life and death. Nat Rev Cancer 9: 738-748, 2009.
7. Liu X, Tang WH, Zhao XM and Chen L: A network approach to predict pathogenic genes for Fusarium graminearum. PLoS One 5: pii: e13021, 2010.
8. Chen L, Wang RS and Zhang XS: Biomolecular networks: Methods and applications in systems biology. John Wiley & Sons, 2009.
9. Ellis JD, Barrios-Rodiles M, Colak R, Irimia M, Kim T, Calarco JA, Wang X, Pan Q, O'Hanlon D, Kim PM, *et al*: Tissue-specific alternative splicing remodels protein-protein interaction networks. Mol Cell 46: 884-892, 2012.
10. Harbison CT, Gordon DB, Lee TI, Rinaldi NJ, Macisaac KD, Danford TW, Hannett NM, Tagne JB, Reynolds DB, Yoo J, *et al*: Transcriptional regulatory code of a eukaryotic genome. Nature 431: 99-104, 2004.
11. Zhang B, Tian Y, Jin L, Li H, Shih IeM, Madhavan S, Clarke R, Hoffman EP, Xuan J, Hilakivi-Clarke L and Wang Y: DDN: A caBIG® analytical tool for differential network analysis. Bioinformatics 27: 1036-1038, 2011.
12. Ma X, Gao L, Karamanlidis G, Gao P, Lee CF, Garcia-Menendez L, Tian R and Tan K: Revealing pathway dynamics in heart diseases by analyzing multiple differential networks. PLoS Comput Biol 11: e1004332, 2015.
13. Kuijjer ML, Rydbeck H, Kresse SH, Buddingh EP, Lid AB, Roelofs H, Bürger H, Myklebost O, Hogendoorn PC, Meza-Zepeda LA and Cleton-Jansen AM: Identification of osteosarcoma driver genes by integrative analysis of copy number and gene expression data. Genes Chromosomes Cancer 51: 696-706, 2012.
14. Ma X, Gao L and Tan K: Modeling disease progression using dynamics of pathway connectivity. Bioinformatics 30: 2343-2350, 2014.
15. Watson-Haigh NS, Kadarmideen HN and Reverter A: PCIT: An R package for weighted gene co-expression networks based on partial correlation and information theory approaches. Bioinformatics 26: 411-413, 2010.

16. Sarawagi S and Kirpal A: Efficient set joins on similarity predicates. In: Proceedings of the 2004 ACM SIGMOD international conference on Management of data ACM, pp743-754, 2004.
17. Benjamini Y and Hochberg Y: Controlling the false discovery rate: a practical and powerful approach to multiple testing. J R Stat Soc. Series B (Methodological) 57: 289-300, 1995.
18. Taylor IW, Linding R, Warde-Farley D, Liu Y, Pesquita C, Faria D, Bull S, Pawson T, Morris Q and Wrana JL: Dynamic modularity in protein interaction networks predicts breast cancer outcome. Nat Biotechnol 27: 199-204, 2009.
19. Bisson N, James DA, Ivosev G, Tate SA, Bonner R, Taylor L and Pawson T: Selected reaction monitoring mass spectrometry reveals the dynamics of signaling through the GRB2 adaptor. Nat Biotechnol 29: 653-658, 2011.
20. Huang da W, Sherman BT and Lempicki RA: Systematic and integrative analysis of large gene lists using DAVID bioinformatics resources. Nat Protoc 4: 44-57, 2009.
21. Huang da W, Sherman BT and Lempicki RA: Bioinformatics enrichment tools: Paths toward the comprehensive functional analysis of large gene lists. Nucleic Acids Res 37: 1-13, 2009.
22. Ciechanover A, Orian A and Schwartz AL: Ubiquitin-mediated proteolysis: Biological regulation via destruction. Bioessays 22: 442-451, 2000.
23. Guo G, Gui Y, Gao S, Tang A, Hu X, Huang Y, Jia W, Li Z, He M, Sun L, *et al*: Frequent mutations of genes encoding ubiquitin-mediated proteolysis pathway components in clear cell renal cell carcinoma. Nat Genet 44: 17-19, 2011.
24. Rivard A, Berthou-Soulie L, Principe N, Kearney M, Curry C, Branellec D, Semenza GL and Isner JM: Age-dependent defect in vascular endothelial growth factor expression is associated with reduced hypoxia-inducible factor 1 activity. J Biol Chem 275: 29643-29647, 2000.
25. Guo M, Cai C, Zhao G, Qiu X, Zhao H, Ma Q, Tian L, Li X, Hu Y, Liao B, *et al*: Hypoxia promotes migration and induces CXCR4 expression via HIF-1α activation in human osteosarcoma. PLoS One 9: e90518, 2014.
26. Nishioka T, Shohag MH, Amano M and Kaibuchi K: Developing novel methods to search for substrates of protein kinases such as Rho-kinase. Biochim Biophys Acta 1854: 1663-1666, 2015.
27. Chiyoda T, Sugiyama N, Shimizu T, Naoe H, Kobayashi Y, Ishizawa J, Arima Y, Tsuda H, Ito M, Kaibuchi K, *et al*: LATS1/WARTS phosphorylates MYPT1 to counteract PLK1 and regulate mammalian mitotic progression. J Cell Biol 197: 625-641, 2012.
28. Li J, Liu X, Liao J, Tian J, Wang J, Wang X, Zhang J and Xu X: MYPT1 sustains centromeric cohesion and the spindle-assembly checkpoint. J Genet Genomics 40: 575-578, 2013.
29. Grassie ME, Moffat LD, Walsh MP and MacDonald JA: The myosin phosphatase targeting protein (MYPT) family: A regulated mechanism for achieving substrate specificity of the catalytic subunit of protein phosphatase type 1δ. Arch Biochem Biophys 510: 147-159, 2011.
30. Lafleur EA, Koshkina NV, Stewart J, Jia SF, Worth LL, Duan X and Kleinerman ES: Increased Fas expression reduces the metastatic potential of human osteosarcoma cells. Clin Cancer Res 10: 8114-8119, 2004.
31. Horowitz JM, Park SH, Bogenmann E, Cheng JC, Yandell DW, Kaye FJ, Minna JD, Dryja TP and Weinberg RA: Frequent inactivation of the retinoblastoma anti-oncogene is restricted to a subset of human tumor cells. Proc Natl Acad Sci USA 87: 2775-2779, 1990.
32. Tanaka M, Setoguchi T, Hirotsu M, Gao H, Sasaki H, Matsunoshita Y and Komiya S: Inhibition of Notch pathway prevents osteosarcoma growth by cell cycle regulation. Br J Cancer 100: 1957-1965, 2009.
33. Ellenbroek SI, Iden S and Collard JG: Cell polarity proteins and cancer. In: Seminars in cancer biology Elsevier, pp208-215, 2012.
34. Vasiliev JM: Cytoskeletal mechanisms responsible for invasive migration of neoplastic cells. Int J Dev Biol 48: 425-440, 2004.
35. Wodarz A and Näthke I: Cell polarity in development and cancer. Nat Cell Biol 9: 1016-1024, 2007.
36. Jaffee EA, Jhaveri DT and Anders R: Diagnostic biomarkers and therapeutic targets for pancreatic cancer. US Patent 20,150,316,554. Filed December 2, 2013; issued November 5, 2015.
37. Phipps KR, Charette J and Baserga SJ: The small subunit processome in ribosome biogenesis-progress and prospects. Wiley Interdiscip Rev RNA 2: 1-21, 2011.
38. Ruggero D and Pandolfi PP: Does the ribosome translate cancer? Nat Rev Cancer 3: 179-192, 2003.
39. Montanaro L, Treré D and Derenzini M: Nucleolus, ribosomes, and cancer. Am J Pathol 173: 301-310, 2008.
40. Kondoh N, Shuda M, Tanaka K, Wakatsuki T, Hada A and Yamamoto M: Enhanced expression of S8, L12, L23a, L27 and L30 ribosomal protein mRNAs in human hepatocellular carcinoma. Anticancer Res 21: 2429-2433, 2001.
41. Jorgensen P, Nishikawa JL, Breitkreutz BJ and Tyers M: Systematic identification of pathways that couple cell growth and division in yeast. Science 297: 395-400, 2002.
42. Bernstein KA and Baserga SJ: The small subunit processome is required for cell cycle progression at G1. Mol Biol Cell 15: 5038-5046, 2004.
43. Colotta F, Allavena P, Sica A, Garlanda C and Mantovani A: Cancer-related inflammation, the seventh hallmark of cancer: Links to genetic instability. Carcinogenesis 30: 1073-1081, 2009.
44. Grivennikov SI, Greten FR and Karin M: Immunity, inflammation, and cancer. Cell 140: 883-899, 2010.
45. Cebola I, Custodio J, Muñoz M, Díez-Villanueva A, Paré L, Prieto P, Aussó S, Coll-Mulet L, Boscá L, Moreno V and Peinado MA: Epigenetics override pro-inflammatory PTGS transcriptomic signature towards selective hyperactivation of PGE2 in colorectal cancer. Clin Epigenetics 7: 74, 2015.
46. Liang Y, Liu M, Wang P, Ding X and Cao Y: Analysis of 20 genes at chromosome band 12q13: RACGAP1 and MCRS1 overexpression in nonsmall-cell lung cancer. Genes Chromosomes Cancer 52: 305-315, 2013.
47. Lomnytska MI, Becker S, Gemoll T, Lundgren C, Habermann J, Olsson A, Bodin I, Engström U, Hellman U, Hellman K, *et al*: Impact of genomic stability on protein expression in endometrioid endometrial cancer. Br J Cancer 106: 1297-1305, 2012.